Talanta 112 (2013) 37–42

Contents lists available at SciVerse ScienceDirect

Talanta

journal homepage: www.elsevier.com/locate/talanta

Colorimetric sensing of copper(II) based on catalytic etching of gold nanoparticles

Ruili Liu [a], Zhaopeng Chen [b,*], Shasha Wang [b,c], Chengli Qu [b], Lingxin Chen [b], Zhuo Wang [a]

[a] School of Environment and Materials Engineering, Yantai University, Yantai 264003, PR China
[b] Key Laboratory of Coastal Zone Environmental Processes, Yantai Institute of Coastal Zone Research (YIC), Chinese Academy of Sciences (CAS); Shandong Provincial Key Laboratory of Coastal Zone Environmental Processes, YICCAS, Yantai 264003, PR China
[c] Graduate University of Chinese Academy of Sciences, Beijing 100049, PR China

ARTICLE INFO

Article history:
Received 21 October 2012
Received in revised form
1 January 2013
Accepted 4 January 2013
Available online 31 March 2013

Keywords:
Gold nanoparticle
Colorimetric
Copper ion
Surface plasmon resonance

ABSTRACT

Based on the catalytic etching of gold nanoparticles (AuNPs), a label-free colorimetric probe was developed for the detection of Cu^{2+} in aqueous solutions. AuNPs were first stabilized by hexadecyltrimethylammonium bromide in NH_3–NH_4Cl (0.6 M/0.1 M) solutions. Then thiosulfate ($S_2O_3^{2-}$) ions were introduced and AuNPs were gradually dissolved by dissolved oxygen. With the further addition of Cu^{2+}, $Cu(NH_3)_4^{2+}$ oxidized AuNPs to produce $Au(S_2O_3)_2^{3-}$ and $Cu(S_2O_3)_3^{5-}$, while the later was oxidized to $Cu(NH_3)_4^{2+}$ again by dissolved oxygen. The dissolving rate of AuNPs was thereby remarkably promoted and Cu^{2+} acted as the catalyst. The process went on due to the sufficient supply of dissolved oxygen and AuNPs were rapidly etched. Meanwhile, a visible color change from red to colorless was observed. Subsequent tests confirmed such a non-aggregation-based method as a sensitive (LOD= 5.0 nM or 0.32 ppb) and selective (at least 100-fold over other metal ions except for Pb^{2+} and Mn^{2+}) way for the detection of Cu^{2+} (linear range, 10–80 nM). Moreover, our results show that the color change induced by 40 nM Cu^{2+} can be easily observed by naked eyes, which is particularly applicable to fast on-site investigations.

1. Introduction

With the development of electronic technology, the global demand of copper is being steadily on the increase. Environmental pollutions resulting from inappropriate disposal of related wastes (e.g. mining residue, smelting slag, electronic trash, etc.) have aroused growing concern over the recent years. It has proven that the excessive accumulation of Cu^{2+} in human bodies has great threat to the nervous system or urinary system [1]. The concentration of Cu^{2+} in drinking water, as recommended by U.S. Environ mental Protection Agency (EPA), should be lower than 1.3 mg/kg (~20 μM) [2]. The detection of Cu^{2+} at such a level or the even lower level, honestly speaking, could be simply achieved in the laboratory by means of mass spectrometry [3], atomic spectroscopy [4], voltammetry [5], etc. However, due to the dependence on sophisticated instruments or the lack of selectivity, none of them could be simplified for the rapid onsite detection of Cu^{2+} in environmental waters. The development of a cost-effective, reliable, and portable method was thus in an urgent need, especially for the environmental monitoring in developing countries and rural regions.

As an easily handled method, the colorimetric method has proven to be practical in the determination of copper in natural waters and foods [6–9]. However, its detection limit was relatively higher due to the low photoabsorption coefficients of Cu-organic complexes. Recent researches show that nanoparticles-based coorimetric assays can overcome the shortcoming of traditional colorimetric methods, since nanoparticles have much higher molar extinction coefficients. Such methods have been succesively developed for the selective and sensitive sensing of proteins [10,11], cells [12,13], DNA[14,15], metal ions [16,17] and anions [18,19]. Corresponding strategies could be divided into three types. One of them was achieved based on the target induced AuNPs aggregation [20,21], where target analytes form complexes with ligands modified on AuNPs' surfaces. This strategy need complicated modifying processes (i.e. label processes) as well as specific equipment (e.g. high speed centrifuges). Another one was based on the AuNPs aggregation resulting from the replacement of stabilizers on AuNPs by target analytes [18,19]. The strategy is relatively simple but suffers from low sensitivity and selectivity. The third one was accomplished by the target induced or target catalyzed etching of AuNPs [22–27]. Such a method is promising due to its simplicity and excellent performance. As compared to

* Corresponding author. Tel./fax: +86 535 2109133.
E-mail address: zhpchen@yic.ac.cn (Z. Chen).

0039-9140/$ - see front matter © 2013 Elsevier B.V. All rights reserved.
http://dx.doi.org/10.1016/j.talanta.2013.01.065

the former two strategies, the last one has been less concerned and applied to only a few analytes.

In our previous work [28], we reported a sensitive and selective colorimetric sensing platform for Cu^{2+} based on the catalytic etching of Au@Ag nanoparticles. Despite its simplicity and performance, the method is still time-consuming (60 min) and not noticeable enough at the level of 100 nM Cu^{2+} for the absorption band of Au@Ag nanoparticles is around 390 nm and very close to the ultraviolet band. In this study, we brought out a much more time-saving and more sensitive to naked-eyes method for the sensing of Cu^{2+}. It is based on the catalytic etching of AuNPs within ammonia medium and the theory could be interpreted as

$$Au+Cu(NH_3)_4^{2+}+5S_2O_3^{2-}\rightarrow Au(S_2O_3)_2^{3-}+Cu(S_2O_3)_3^{5-} \quad (1)$$

and

$$Cu(S_2O_3)_3^{5-}+O_2+16NH_3+4H^+\rightarrow 4Cu(NH_3)_4^{2+}+5S_2O_3^{2-} \quad (2)$$

Following the method, a noticeable color change induced by 40 nM Cu^{2+} would occur within 25 min.

2. Experimental

2.1. Chemicals and apparatus

Hydrogen tetrachloroaurate(III) dehydrate, trisodium citrate, sodium thiosulfate and hexadecyltrimethylammonium bromide (CTAB) were obtained from Sinopharm® Chemical Reagent (China). All other chemicals were analytical reagent grade or better. Solutions were prepared with deionized water (18.2 MΩ, Pall® Cascada). Absorption spectra of AuNPs were scanned by the UV/visible spectrophotometer (Beckman Coulter® DU-800, USA). Images of dispersed AuNPs were achieved by transmission electron microscopy (TEM, JEOL® JEM-1230, Japan) operated at 100 kV. Dynamic light scattering (DLS) tests were performed on a Zeta Potential/Particle Sizer (Malven® Nano ZS-90, UK).

2.2. Methods

2.2.1. Gold nanoparticles synthesis

Citrate-capped gold nanoparticles were prepared according to the Frens' method by means of the chemical reduction of $HAuCl_4$ by citrate in the liquid phase [29]. Briefly, 200 mL aqueous solution of 1 mM $HAuCl_4$ was first brought to boil with vigorous stirring. Then 20 mL trisodium citrate with a concentration of 38.8 mM was added rapidly and the mixture was heated under reflux for another 10 min. During the process, the color changed from pale yellow to deep red. Thereafter, the solution was cooled to room temperature while being stirred continuously. The size of AuNPs, as determined by TEM imaging, was 15 nm.

2.2.2. Sensing procedure

To 200 μL AuNPs, 10 μL CTAB (0.1 M) was firstly added to ensure AuNPs stable in a NH_3–NH_4Cl (0.6 M/0.1 M) solution. After thorough mixing, the colloidal solution was further mixed with 800 μL NH_3–NH_4Cl buffer solution containing different amount of Cu^{2+}. Then 5 μL $Na_2S_2O_3$ with a concentration of 1.0 M was added and the solution was incubated at 70 °C for 25 min. The absorption spectra of final solutions were recorded.

2.2.3. Analysis of real samples

Local shellfish samples were wet digested for analyses. Briefly, the tissues were washed with deionized water thoroughly and then frozen at −28 °C. They were subsequently freeze-dried and ground to powders for digestion. To 0.3 g powder sample, 10 mL ultrapure HNO_3 were added and the mixtures were digested in a high pressure tank at 150 °C for 6 h. Digestive solutions were further diluted to 50 mL for use.

For sample analysis, different volumes of above diluted samples, tap water (obtained from our institute) or local drinking water, 5 μL $Na_2S_2O_3$ (1.0 M), and 200 μL CTAB stabilized AuNPs were successively added to 800 μL NH_3–NH_4Cl buffers. The solutions were incubated at 70 °C for 25 min before recording the absorption spectra. The concentrations of Cu^{2+} were calculated by the calibration curve.

3. Results and discussion

3.1. Mechanism of the sensor

The ionic system of $S_2O_3^{2-}$–Cu^{2+} has been applied to extraction of gold from ores for many years. In this system, Cu^{2+} first reacted with NH_3 to form $Cu(NH_3)_4^{2+}$ complexes. Then $Cu(NH_3)_4^{2+}$ oxidized gold in the presence of $S_2O_3^{2-}$ to produce water-soluble $Au(S_2O_3)_2^{3-}$ and $Cu(S_2O_3)_3^{5-}$. $Cu(S_2O_3)_3^{5-}$ was converted to $Cu(NH_3)_4^{2+}$ again by dissolved oxygen. During the whole process, Cu^{2+} acted as a catalyst and had not been consumed. The related thermodynamic data are displayed as follows [30], where φ^{θ} represents the standard potential.

$$Cu(NH_3)_4^{2+}+3S_2O_3^{2-}+e\rightarrow Cu(S_2O_3)_3^{5-}+4NH_3\ \varphi^{\theta}=0.22\ V\ vs\ NHE \quad (3)$$

$$Au(S_2O_3)_2^{3-}+e\rightarrow Au+2S_2O_3^{2-}\ \varphi^{\theta}=0.15V\ vs\ NHE \quad (4)$$

$$O_2+H_2O+4e\rightarrow 4OH^-\ \varphi^{\theta}=0.40\ V\ vs\ NHE \quad (5)$$

Scheme 1 outlines the sensing mechanism of this study. When CTAB stabilized AuNPs reacted with $S_2O_3^{2-}$, $Au(S_2O_3)_2^{3-}$ complexes were formed and AuNPs were partly dissolved (gold can be leached slowly by O_2 in the presence of $S_2O_3^{2-}$ [31]). The SPR absorption of AuNPs thereby decreased. Once Cu^{2+} was introduced, the dissolving process was greatly accelerated and the color of solution faded rapidly.

To verify the role of Cu^{2+} as a catalyst in the etching of AuNPs, the SPR absorption spectra of AuNPs were monitored (Fig. 1). Curve a displayed the absorption spectrum of CTAB stabilized

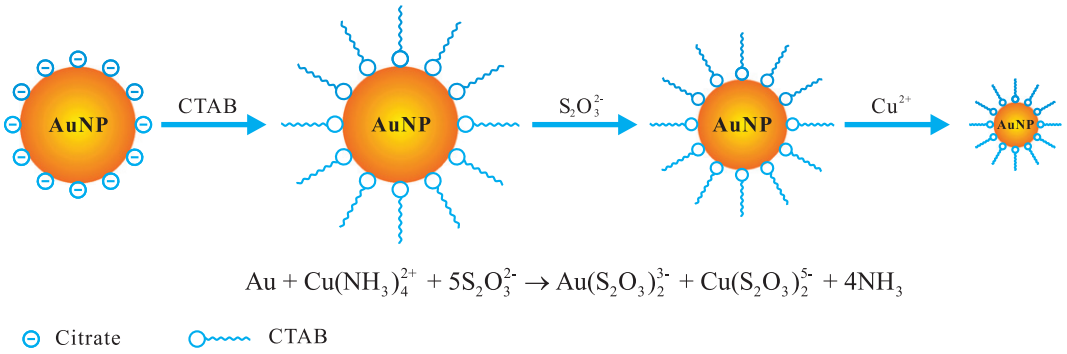

Scheme 1. Schematic illustration for the colorimetric sensing of Cu^{2+} based on etching of AuNPs .

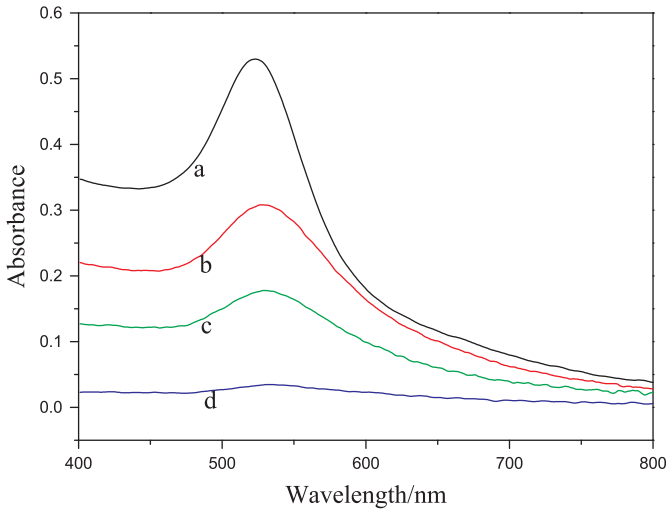

Fig. 1. The absorption spectra of CTAB stabilized AuNPs (a) and after incubation with 5.0 mM $S_2O_3^{2-}$ (b), 5.0 mM $S_2O_3^{2-}$+0.04 μM Cu^{2+} (c), 5.0 mM $S_2O_3^{2-}$+0.1 μM Cu^{2+} (d), respectively.

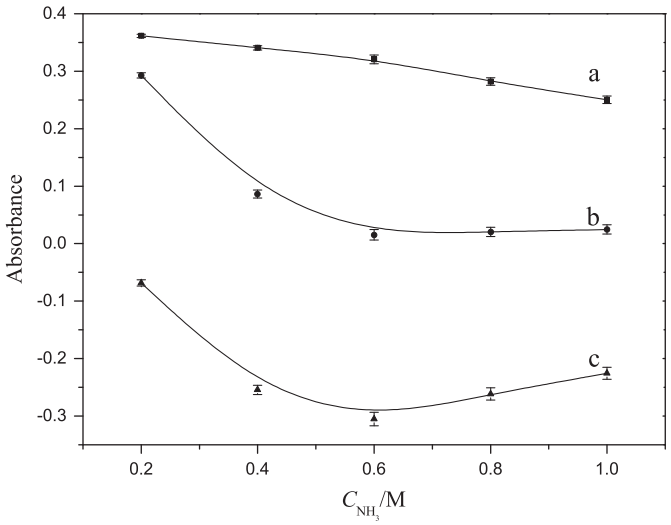

Fig. 2. Absorbance of AuNPs at 527 nm after incubation with 5.0 mM $S_2O_3^{2-}$ (curve a), 5.0 mM $S_2O_3^{2-}$+0.1 μM Cu^{2+} (b), and Δ_A (c) in different concentration of NH_3 at 70 °C for 30 min.

AuNPs and the strongest SPR absorption appeared at 521 nm. The addition of $S_2O_3^{2-}$ caused the absorption at 521 deceased to ~2/3 (curve b), accompanied by a slight red-shift of the absorption peak from 521 to 527 nm. The DLS results showed that the diameters of CTAB stabilized AuNPs before and after addition of $S_2O_3^{2-}$ were 16.15 and 15.14 nm, respectively. Hence, the intensity decrease of the SPR absorption could be attributed to the shrink of particles sizes. The SPR absorption spectra of AuNPs decreased dramatically in the presence of Cu^{2+} (Fig. 1, curve c and d). The DLS results revealed that Cu^{2+} at the level of 0.04 and 0.1 μM would reduce the diameters of CTAB stabilized AuNPs to 12.09 and 11.64 nm, respectively. It suggests that the etching of AuNPs were accelerated by the co-work of Cu^{2+} and $S_2O_3^{2-}$. It is noteworthy that almost no AuNPs <8 nm were found in the remaining solution, since such AuNPs are even easier to be leached by oxidants such as dissolved oxygen and Cu^{2+}.

3.2. Optimize the sensing conditions

Since our method is based on the catalytic leaching of AuNPs, the optimization of experimental conditions is very necessary. Factors to be tested include the concentrations of NH_3 and $S_2O_3^{2-}$, the incubation temperature and time. With respect to the fact that AuNPs would also be etched by dissolved oxygen in the absence of Cu^{2+}, the difference between the absorbance of AuNPs before and after addition of Cu^{2+} ($\Delta_A = A_{sample} - A_{blank}$) was chosen as a reference for optimization.

3.2.1. Effect of the concentration of NH_3

The effect of NH_3 on the leaching of AuNPs was investigated in the absence and presence of Cu^{2+} (0.1 μM), while other factors were fixed (NH_4Cl=0.1 M, $S_2O_3^{2-}$=5.0 mM, incubation temperature=70 °C and time=30 min). As shown in Fig. 2, in the absence of Cu^{2+}, the absorbance of AuNPs at 527 nm decreased slightly with the increase of NH_3 (curve a). The slight decrease can be attributed to the increase of conditional stability constant of $Au(S_2O_3)_2^{3-}$ with pH increasing and consequent decrease of the practical redox potential of $Au(S_2O_3)_2^{3-}$/Au. However, in the presence of Cu^{2+} (curve b), the absorbance of AuNPs at 527 nm decreased dramatically with the increase of NH_3 from 0.2 to 0.6 M, since more $Cu(NH_3)_4^{2+}$ were formed in the solution. Further addition of $NH_3 > 0.6$ M almost yielded no more effects. The Δ_A reached its lowest value and kept stable when the concentration of NH_3 was set at 0.6 M. To achieve high sensitivity, a concentration of 0.6 M was selected in following experiments.

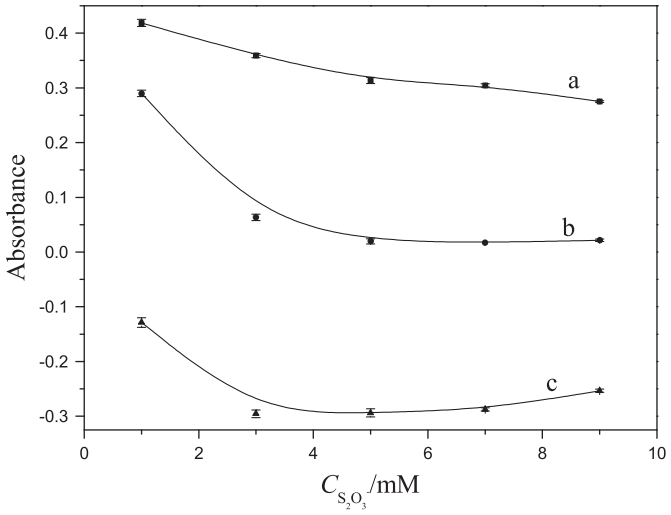

Fig. 3. Absorbance of AuNPs at 527 nm after incubation with NH_4Cl–NH_3 (0.1/0.6 M) buffer solution containing different concentration of $S_2O_3^{2-}$ with the absence (a), presence of 0.1 μM Cu^{2+} (b) and Δ_A (c) at 70 °C for 30 min.

3.2.2. Effect of the concentration of $S_2O_3^{2-}$

Fig. 3 showed the effect of $S_2O_3^{2-}$ on the leaching of AuNPs. In the absence of Cu^{2+} (curve a), the absorbance of AuNPs at 527 nm decreased slightly with the increase of $S_2O_3^{2-}$. In the presence of Cu^{2+} (curve b), the absorbance decreased sharply with the increase of $S_2O_3^{2-}$ from 1.0 to 5.0 mM. It should be attributed to both the decrease in practical redox potential of $Au(S_2O_3)_2^{3-}$/Au and the increase in the redox potential of $Cu(NH_3)_4^{2-}$/$Cu(S_2O_3)_3^{5-}$. However, the effect would not be remarkably promoted when $S_2O_3^{2-}$ exceeded 5.0 mM. The Δ_A reached its lowest value when the concentration of $S_2O_3^{2-}$ was set at 5.0 mM (curve c). As a result, $S_2O_3^{2-}$ with a concentration of 5.0 mM was chosen in following experiments.

3.2.3. Effect of the incubation temperature and time

Figs. 4 and 5 showed the effects of incubation temperature and time. In the absence of Cu^{2+} (curve a in two figures), both of them showed insignificant effects. As compare, the absorbance of AuNPs at 527 nm would decrease sharply with the increase of temperature (within 70 °C) or time (within 25 min). The incubation temperature of 70 °C and the incubation time of 25 min were thereby selected.

3.3. Selectivity of the sensor

To test the selectivity of our sensor, various environmentally relevant ions were added to the solution separately. The inset in Fig. 6 shows the presence of Cu^{2+} (0.1 μM) turned the AuNPs to almost colorless and a remarkable decrease of the absorbance at 527 nm was observed (Fig. 6). As compare, the existence of about 100-fold excess of Mg^{2+}, Ag^{+}, Li^{+}, Na^{+}, Hg^{2+}, As(V), Co^{2+}, Cd^{2+}, Fe^{3}

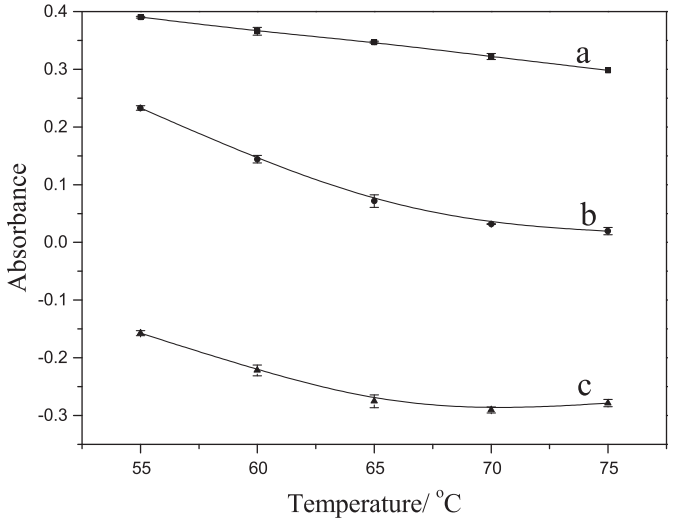

Fig. 4. Absorbance of AuNPs at 527 nm after incubation with NH_4Cl–NH_3 (0.1/0.6 M) buffer solution containing 5.0 mM $S_2O_3^{2-}$ with the absence (a), presence of 0.1 μM Cu^{2+} (b) and Δ_A (c) at different temperature for 30 min.

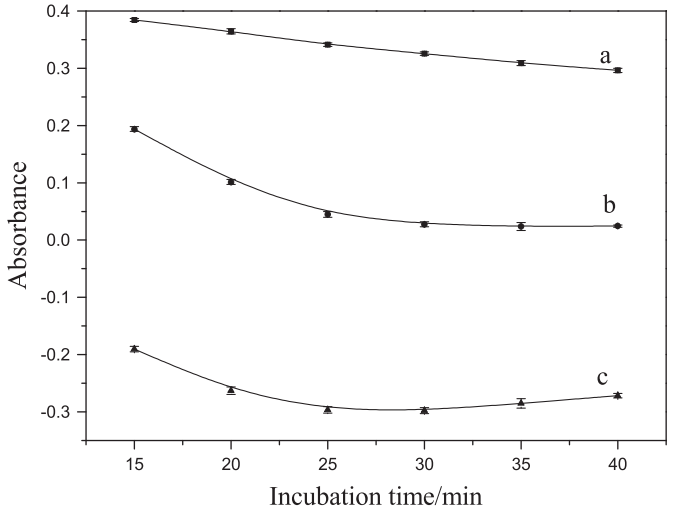

Fig. 5. Absorbance of AuNPs at 527 nm after incubation with NH_4Cl–NH_3 (0.1/0.6 M) buffer solution containing 5.0 mM $S_2O_3^{2-}$ with the absence (a), presence of 0.1 μM Cu^{2+} (b) and Δ_A (c) at 70 °C for different time.

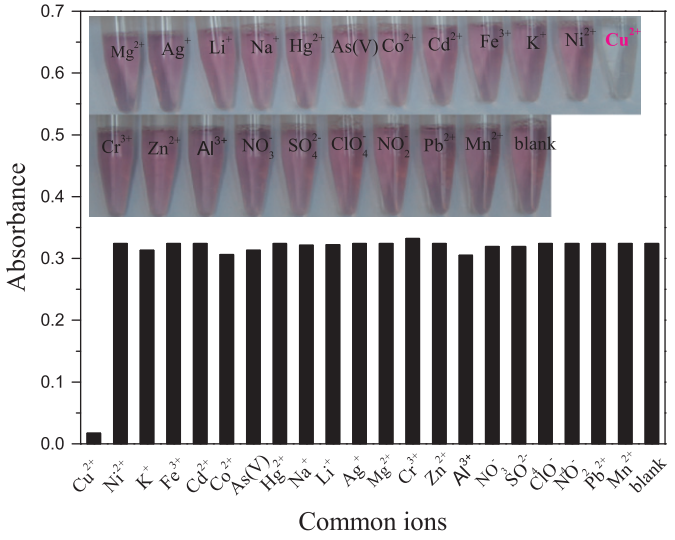

Fig. 6. Absorbance at 527 nm and color of AuNPs after incubation with NH_4Cl–NH_3 (0.1/0.6 M) buffer solution in the presence of common ions with a concentration of 10 μM (except 0.1 μM Cu^{2+}, 0.1 μM Mn^{2+} and 1 μM Pb^{2+}) containing 5.0 mM $S_2O_3^{2-}$ at 70 °C for 25 min.

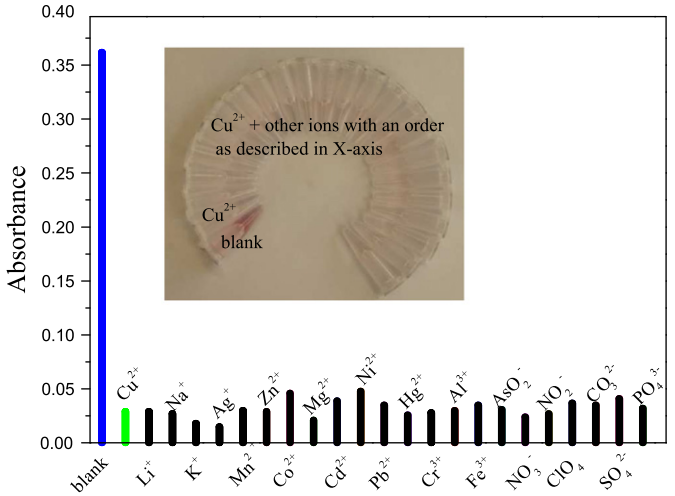

Fig. 7. Influence of common ions with a concentration of 10 μM (except 0.1 μM Mn^{2+} and 1 μM Pb^{2+}) on the determination of 0.1 μM Cu^{2+}. Blue bare: absorbance response of the probe to blank; green bar: absorbance response of the probe to 0.1 μM Cu^{2+}; black bar: absorbance response of the probe to 0.1 μM Cu^{2+} in the presence of other ions. (For interpretation of the references to color in this figure legend, the reader is referred to the web version of this article.)

$^{+}$, K^{+}, Ni^{2+}, Cr^{3+}, Zn^{2+}, Al^{3+}, NO_3^{-}, SO_4^{2-}, ClO_4^{-} and NO_2^{-}, 10-fold of Pb^{2+} and same concentration of Mn^{2+} caused almost no noticeable color change. The absorbance of AuNPs at 527 nm ($A_{527\ nm}$) with the addition of above ions remained similar to that yielded by the blank. The proposed method was confirmed with excellent selectivity toward Cu^{2+}.

3.4. Interference

The interference of other environmentally relevant ions were also investigated by addition of relevant ions separately to Cu^{2+}-containing solution before incubation under 70 °C. As shown in Fig. 7, the coexistence of 100-fold excess of Mg^{2+}, Ag^{+}, Li^{+}, Na^{+}, Hg^{2+}, As(V), Co^{2+}, Cd^{2+}, Fe^{3+}, K^{+}, Ni^{2+}, Cr^{3+}, Zn^{2+}, Al^{3+}, NO_3^{-}, SO_4^{2-}, ClO_4^{-} and NO_2^{-}, PO_4^{3-}, CO_3^{2-}, AsO_2^{-}, 10-fold of Pb^{2+} and same concentration of Mn^{2+} had little effect on the determination of Cu^{2+}.

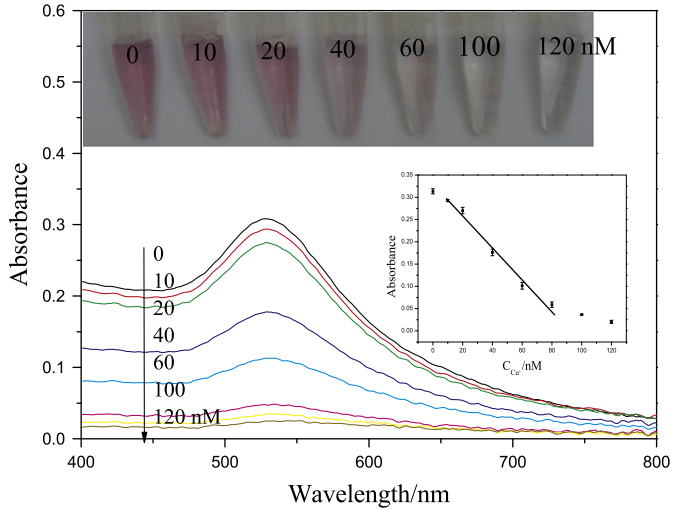

Fig. 8. Absorption spectra of AuNPs after incubation with different concentrations of Cu^{2+} in NH_4Cl–NH_3 (0.1/0.6 M) buffer solution containing 5.0 mM $S_2O_3^{2-}$ at 70 °C for 25 min. Insets show the absorbance response to different concentrations of Cu^{2+} and the color change with the increase of Cu^{2+} concentration from left to right. (For interpretation of the references to color in this figure legend, the reader is referred to the web version of this article.)

Table 1
Comparison of the sample analysis results obtained by ICP-MS and proposed method.

Shellfish samples	Found by ICP-MS/μM	Found by proposed method/μM	Recoveries (%)
Shellfish samples 1	6.70	8.3 ± 0.3	124 ± 3.6
Shellfish samples 2	2.15	2.6 ± 0.1	121 ± 4.7
Shellfish samples 3	10.0	7.5 ± 0.2	75 ± 2.0
Shellfish samples 4	7.18	7.1 ± 0.4	99 ± 5.6
Shellfish samples 5	3.58	3.3 ± 0.2	92 ± 5.6
Tap water	2.06	1.89 ± 0.2	91.7 ± 10
Drinking water	4.12	3.76 ± 0.5	91.3 ± 12

The result was also confirmed by the digital photo (the inset in Fig. 7).

3.5. Sensitivity of the sensor

To evaluate the sensitivity of the sensor, the UV–vis spectra of AuNPs solutions in the presence of various concentrations of Cu^{2+} under the optimized conditions were recorded. The absorbance at 527 nm versus the concentration of Cu^{2+} was plotted as Fig. 8 It is obvious that the A_{527} nm value gradually decreased with the increase of Cu^{2+}. A good linear relationship between the $A_{527\ nm}$ and Cu^{2+} concentrations was obtained within the range of 10.0 to 80 nM ($R^2 = 0.990$). The detection limit was calculated to be 5.0 nM, which is far below the maximum containment level as recommended by U.S. EPA (~20 μM). The digital photo in the inset of Fig. 7 indicates that a containment level of 40 nM Cu^{2+} (~2.6 ppb) can be easily read out by naked eyes.

3.6. Sample analysis

The practical performance of proposed method was further tested by sensing of Cu^{2+} in digested shellfish, tap and drinking water samples. The results were consistent with those obtained by ICP-MS, indicating the method is applicable to the quantification of Cu^{2+} in real samples. The applicability was also supported by similar comparative analyses of digested water samples (Table 1).

4. Conclusions

In summary, we developed a new rapid colorimetric assay for the sensitive and selective detection of Cu^{2+} based on the catalytic etching of AuNPs. The changes in the SPR absorptions of AuNPs yield a rapid method for the inspection of Cu^{2+} in aqueous solutions. Under the optimized conditions, the Cu^{2+}-specific probe exhibits high sensitivity towards Cu^{2+} but also high selectivity over other possible interference ions. The method is also highlighted by its simplicity and rapidity as compared to many other nanoparticles-based colorimetric methods [32–41]. Compared with our former research [28], the present work is more time-saving and sensitive to naked-eyes. The color change induced by Cu^{2+} as low as 40 nM is remarkable enough to be observed by naked eyes. With respect to above advantages, we consider that the proposed the sensing system of Cu^{2+} has considerable applicability to field investigations, especially for the preparation of economical Cu^{2+} test papers

Acknowledgments

The research was financially supported by the Department of Science and Technology of Shandong Province (BS2009DX006, 2008GG20005005),NSFC (no. 21275158), CAS (KZCX2-YW-JS208) and the 100 Talents Program of the CAS.

References

[1] V. Desai, S.G. Kaler, Am. J. Clin. Nutr. 88 (2008) 855S–858S.
[2] Y.T. Su, G.Y. Lan, W.Y. Chen, H.T. Chang, Anal. Chem. 82 (2010) 8566–8572.
[3] J.S. Becker, A. Matusch, C. Depboylu, J. Dobrowolska, M.V. Zoriy, Anal. Chem. 79 (2007) 6074–6080.
[4] E.S. Dipietro, M.M. Bashor, P.E. Stroud, B.J. Smarr, B.J. Burgess, W.E. Turner, J.W. Neese, Sci. Total Environ. 74 (1988) 249–262.
[5] A.M. Beltagi, M.M. Ghoneim, J. Appl. Electrochem. 39 (2009) 627–636.
[6] X. Liao, B. Liang, Z. Li, Y. Li, Analyst 136 (2011) 4580–4586.
[7] J. Lima, C. Delerue-Matos, M. Vaz, Food Chem. 62 (1998) 117–121.
[8] T. Makino, J.I. Itoh, Clin. Chim. Acta 111 (1981) 1–8.
[9] O. Ozcan, M. Gultepe, O.M. Pcolu, E. Cakir, Clin. Chem. 52 (2006) A182-A182.
[10] D. Aili, R. Selegard, L. Baltzer, K. Enander, B. Liedberg, Small 5 (2009) 2445–2452.
[11] G. Liang, S. Cai, P. Zhang, Y. Peng, H. Chen, S. Zhang, J. Kong, Anal. Chim. Acta 689 (2011) 243–249.
[12] W. Lu, S.R. Arumugam, D. Senapati, A.K. Singh, T. Arbneshi, S.A. Khan, H. Yu, P.C. Ray, ACS Nano 4 (2010) 1739–1749.
[13] C.D. Medley, J.E. Smith, Z. Tang, Y. Wu, S. Bamrungsap, W. Tan, Anal. Chem. 80 (2008) 1067–1072.
[14] M.S. Han, A.K. Lytton-Jean, B.K. Oh, J. Heo, C.A. Mirkin, Angew. Chem. Int. Ed. Engl. 45 (2006) 1807–1810.
[15] S.J. Hurst, M.S. Han, A.K.R. Lytton-Jean, C.A. Mirkin, Anal. Chem. 79 (2007) 7201–7205.
[16] Y. Wang, F. Yang, X. Yang, Biosens. Bioelectron. 25 (2010) 1994–1998.
[17] G. Wang, Y. Wang, L. Chen, J. Choo, Biosens. Bioelectron. 25 (2010) 1859–1868.
[18] Z. Zhang, J. Zhang, C. Qu, D. Pan, Z. Chen, L. Chen, Analyst 137 (2012) 2682–2686.
[19] C.Y. Liu, W.L. Tseng, Chem. Commun. 47 (2011) 2550–2552.
[20] A. Alizadeh, M.M. Khodaei, C. Karami, M.S. Workentin, M. Shamsipur, M. Sadeghi, Nanotechnology 21 (2010) 315503.
[21] M. Zhang, Y.-Q. Liu, B.-C. Ye, Chem. Commun. 47 (2011) 11849–11851.
[22] S.K. Tripathy, J.Y. Woo, C.-S. Han, Anal. Chem. 83 (2011) 9206–9212.
[23] Y.Y. Chen, H.T. Chang, Y.C. Shiang, Y.L. Hung, C.K. Chiang, C.C. Huang, Anal. Chem. 81 (2009) 9433–9439.
[24] F.M. Li, J.M. Liu, X.X. Wang, L.P. Lin, W.L. Cai, X. Lin, Y.N. Zeng, Z.M. Li, S.Q. Lin, Sens. Actuators B Chem. 155 (2011) 817–822.
[25] R.X. Zou, X. Guo, J. Yang, D.D. Li, F. Peng, L. Zhang, H.J. Wang, H. Yu, CrystEngComm 11 (2009) 2797–2803.
[26] L. Shang, L. Jin, S. Dong, Chem. Commun. 21 (2009) 3077–3079.
[27] Y. Fan, Z. Liu, L. Wang, J. Zhan, Nanoscale Res. Lett. 4 (2009) 1230–1235.
[28] T. Lou, L. Chen, Z. Chen, Y. Wang, L. Chen, J. Li, ACS Appl. Mater. Interfaces 3 (2011) 4215–4220.

[29] G. Frens, Nat. Phys. Sci 241 (1973) 20–22.
[30] P.L. Breuer, M.I. Jeffrey, Hydrometallurgy 65 (2002) 145–157.
[31] G. Senanayake, Hydrometallurgy 77 (2005) 287–293.
[32] S.K. Tripathy, J.Y. Woo, C.S. Han, Nanotechnology 23 (2012) 305502.
[33] Y.F. Lee, T.W. Deng, W.J. Chiu, T.Y. Wei, P. Roy, C.C. Huang, Analyst 137 (2012) 1800–1806.
[34] C. Hua, W.H. Zhang, S.R.M. De Almeida, S. Ciampi, D. Gloria, G. Liu, J.B. Harper, J.J. Gooding, Analyst 137 (2012) 82–86.
[35] E. Oliveira, J. Dinis Nunes-Miranda, H.M. Santos, Inorg. Chim. Acta 380 (2012) 22–30.
[36] Y. Guo, Z. Wang, W. Qu, H. Shao, X. Jiang, Biosens. Bioelectron. 26 (2011) 4064–4069.
[37] X. Zhang, X. Kong, W. Fan, X. Du, Langmuir 27 (2011) 6504–6510.
[38] P. Yang, Y. Zhao, Y. Lu, Q.Z. Xu, X.W. Xu, L. Dong, S.H. Yu, ACS Nano 5 (2011) 2147–2154.
[39] Y. Wang, F. Yang, X. Yang, Nanotechnology 21 (2010) 205502.
[40] X.R. He, H.B. Liu, Y.L. Li, S. Wang, Y.J. Li, N. Wang, J.C. Xiao, X.H. Xu, D.B. Zhu, Adv. Mater. 17 (2005) 2811–2825.
[41] N. Ratnarathorn, O. Chailapakul, C.S. Henry, W. Dungchai, Talanta 99 (2012) 552–557.